

PROBABILISTIC APPROACH TO DETERMINATION OF INTERNAL HEAT GAINS IN OFFICE BUILDING FOR PEAK LOAD CALCULATIONS

Tatsuo Nagai¹ and Akihiro Nagata²

¹ Tokyo University of Science, Tokyo, Japan

² Tokyo Metropolitan University, Tokyo, Japan

ABSTRACT

We propose a methodology for determining internal heat gains in workspace for peak cooling/heating load calculations. First, we collected measurement data of the lighting and plug loads in workspaces in Japan and analyzed these data. The investigation results show that internal heat gains remain relatively flat during work hours for each space, but their magnitudes vary considerably from space to space. Time-averaged heat gains during work hours conform to a lognormal distribution if those spaces are approximately the same size in floor area. Next, we present a methodology to determine the value of heat gains at specified frequencies of occurrence for each space. We present detailed procedures to calculate the probabilistic distributions with the Markov chain Monte Carlo method in conjunction with the Bayesian approach and analyze the calculation results by using the measured data. Finally, we discuss the applicability of the proposed stochastic approach.

INTRODUCTION

Peak load calculations are carried out to determine the capacity of air handling units, pumps, chillers, and every other component of an HVAC system. Climate conditions and internal heat gains are major uncertainty factors that affect the peak load. Usually, individual countries prepare peak design weather data that occur at a specific frequency. Peak internal heat gains, in contrast, are commonly presented as deterministic value, and seldom defined according to their stochastic nature.

For example, 2009 ASHRAE Handbook - Fundamentals, lists recommended load factors for several load density such as "Light" or "Medium" in deterministic way (e.g., 10.8 W/m² for "Medium" density). Wilkins, 1998 measured electric power for each piece of equipment as well as the total plug load of the space. The results show the usage diversity, i.e., the ratio of the measured total plug load of the space to the total maximum possible power for each piece of equipment, is approximately 50%. Considering that the usage diversity is less than 1 because of the gap of time during which each equipment is in operation with maximum power, the peak internal heat gains per floor area of a space should decrease

with increase of the floor area due to the load leveling. However, the relationship between the peak internal heat gains and the floor area has remained unclear.

Pedersen, 2007, Pedersen et al., 2008 developed a new method for load modelling of buildings in mixed energy distribution systems. The method aggregates individual building load profiles to derive the load profile for a specified planning area under the assumption that the load profiles for different building categories are independent. The author noted that the correlation between each building's load demand has little influence on the resulting aggregated load. However, there is a possibility that electricity load for a particular space correlates with the load of the adjacent space in the same building.

There are other literatures on day-to-day variations of internal heat gain for each building (Abushakra et al., 2001, Saldanha et al., 2012), but the authors could not find previous research that focuses on quantitative analysis of space-to-space variations in a building in the absence of information about the type and the number of installed equipment in the target space.

This paper presents a probabilistic approach to determine design conditions for internal heat gains in an office building for peak load calculations. The design conditions for heat gains can differ according to the target floor area; for example, the peak design heat gains for selecting chillers could be smaller than those for selecting air handling units because chillers cover a much larger area than do air handlers. The derived chart that illustrates percentiles of internal heat gain at a specified floor area gives opportunity for equalizing exceedance probability of overload for each HVAC equipment. Especially, the chiller capacity could be reduced by the derived chart, and it might lead to reduction of construction cost and improvement of the efficiency of the chiller due to higher load ratio through the year.

In this paper, we firstly collect measurement data of the lighting and plug loads in workspaces in Japan. The variability of internal heat gains generally consists of two factors: the variation associated with the difference in spaces, and the diurnal variation in a space. We analyze the collected data and show the dominating factor.

Next, we present a methodology to derive a specific percentile of heat gains for each floor space area. We employ the Bayesian method with the Markov chain Monte Carlo (MCMC) method to determine the parameters for the probabilistic distributions of internal heat gains for a specified floor area.

Finally, we analyze the calculation results by using the measured data, and discuss the applicability of the proposed stochastic approach.

OBSERVATIONS OF INTERNAL HEAT GAINS

Data source

We collected hourly observation data of the electricity consumption in workspaces in office buildings in Japan (Refer to SHASE, 2011). Some of the data were measured by the authors, and the remaining were collected from other literature sources. Table 1 shows an outline of the data. “No.” in the table refers to a literature source reported by each author(s). Each report targets one building except report No.11, which targets 4 buildings. In this paper, each report is referred to by a building number (for example, “Building No.2” refers to the report No.2) if not otherwise specified.

The target spaces include meeting space, walking space, and workspace, but do not include corridors, restrooms, staircases, etc., in the common space. The spaces vary from approximately 150 to 1600 m². There were three ways of measurements: (1) plug loads were measured separately from lighting load, (2) the total lighting and plug loads was measured, (3) only plug loads were measured. The data for analyzing the total lighting and plug loads are gathered from measurements in the first two cases, i.e., case (1) and case (2). Analyses on plug loads are carried out by using the data in case (1) and (3). The total number of measured spaces is 35 for analyzing the total lighting and plug loads, and 42 for the plug loads. The years in which measurements were carried

out ranged from 2004 to 2010.

Variation of plug loads (Building No. 2)

Figure 1 shows the diurnal variation of the plug loads in Building No. 2 on one day of weekday. In this building, plug loads are measured separately in three spaces on both the 4th and 5th floors. From Figure 1, we find that the plug load varies from space to space. The areas of those spaces are 289, 167, and 247m². (The total is 703 m² for each floor, which is the value appeared in Table 1. The total plug loads over each floor are analyzed since the next section.) The variability of plug loads tends to be large because the facility layout greatly affects the plug load per area in such small spaces.

Figure 2 shows the differences on three days in the plug loads of the “Center” space, which is one of the three spaces on each floor. The differences between days are small compared to the variation from space to space. Moreover, the time variation is rather small during work hours.

To summarize, the variation from space to space is large, especially in small spaces, but both the time variation during work hours and the daily variation is rather small.

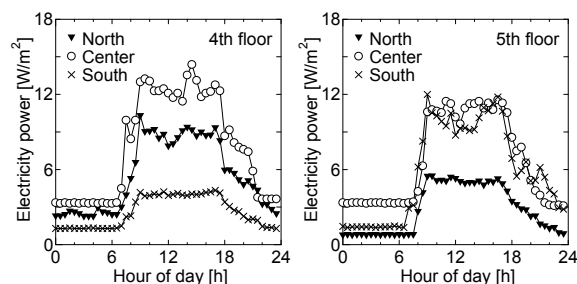


Figure 1 Differences in plug load in three spaces (Nov. 4, Building No. 2)

Table 1 Outline of measured data (SHASE, 2011)

Report No.	Total lighting and plug loads					Plug load					Reference
	Number of spaces	Area [m ²]	Collection method*1	Sampling interval	Measurement period	Number of spaces	Area [m ²]	Collection method*1	Sampling interval	Measurement period	
1	16	250-290	B	1h	7/1-7/31, 2009	2	525	I*2	1h	9/1,2008-2/28,2009	SHASE, 2011
2	2	703	I*3	30min	3/31,7/29,11/4,2004	2	703	C	30sec	11/1-11/6, 2004	SHASE, 2008
3	5	420	B	1min	2006 (Whole year)	-	-	-	-	-	SHASE, 2008
4	5	792-1602	B	1h	2003 (Whole year)	1	792	I*2	1h	8/19-9/24, 2004	SHASE, 2008
5	1	800	C	unknown	2006-2007	1	800	C	unknown	2006-2007	SHASE, 2008
6	-	-	-	-	-	26	200-840	C	1min	1/8-2/26, 2005*4	Kawase, 2005
7	1	765	C	10min	11/17-12/9, 2009	1	765	C	10min	11/17-12/9, 2009	Tokyo Denki Univ., 2010
8	1	553	C	10min	12/17-12/25, 2009	1	553	C	10min	12/17-12/25, 2009	Tokyo Denki Univ., 2010
9	2	350-393	C	10min	11/9-11/15, 2009	2	350-393	C	10min	11/9-11/15, 2009	Tokyo Denki Univ., 2010
10	1	149	C	10min	1/28-2/3, 2010	1	149	C	10min	1/28-2/3, 2010	Tokyo Denki Univ., 2010
11	1	197	C	1min*5	unknown	3	197-497	C	1min	unknown	Shinkawa, 2006
12	-	-	-	-	-	1	475	C	1min	7/11, 2003-1/30, 2004	Akiba, 2004
13	-	-	-	-	-	1	473	C	1min	9/29-12/22, 2004	Akiba, 2005
Total	35	-	-	-	-	42	-	-	-	-	-

*1 B: Collected by building energy management system, C: Collected by data acquisition logger (temporarily installed), I: Integrated method

*2 Plug load are derived by subtracting lighting load measured by dedicated sensor from total lighting and plug loads measured by BEMS

*3 Lighting load are estimated by multiplying lighted ratio checked at 30min intervals by rated power consumption. Plug load are collected by sensor.

*4 Measurement period for each space is 1 week

*5 Sampling interval for plug load (sampling interval for lighting load unknown)

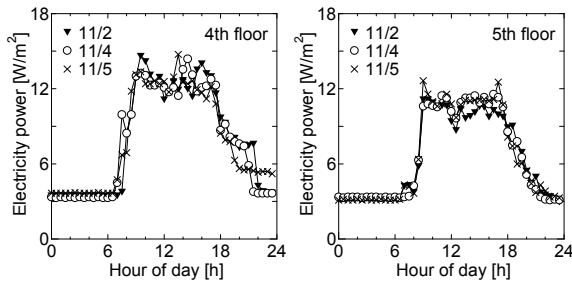


Figure 2 Differences in plug load on three days (Center, Building No. 2)

Reduction in variation due to increase of floor area (Building No. 2)

Figure 3 shows the mean and the standard deviation (S.D.) of internal heat gains in Building No. 2. Those statistics are derived by using the hourly data of three weekdays from 9 a.m. to 5 p.m. (except the lunch hour). We count the number of persons every hour in each target space by visual inspection, and assume 110 W/person to estimate the heat gain for each space.

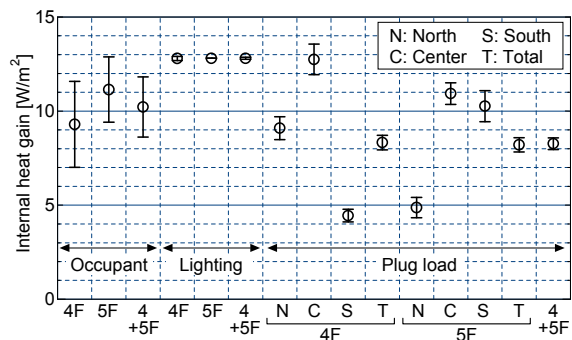


Figure 3 Daytime means and standard deviations of internal heat gains (Building No. 2)

The mean of the lighting load is approximately 13 W/m², and the S.D. is very small because almost all lighting switches were turned on during work hours. The S.D.s of the occupants are larger than those of the lighting or plug loads. The S.D. of the occupants of the 4th and 5th floors combined is not less than that of either the 4th or 5th floor, even though the area is double.

The means of the plug loads greatly differ from space to space, but the mean for the 4th floor is approximately the same as that for the 5th floor. That suggests the variation in the mean decreases with the increase of floor area.

Diurnal variation and daytime average (all buildings)

Figure 4 (left) shows the averaged diurnal variations of each measured space. Basically, heat gains remain flat during work hours except during the lunch hour. Thus, we assume the peak heat gain of each

measured area can be estimated approximately by averaging over these periods.

Figure 4 (right) shows the relationship between the time-averaged daytime heat gain and the floor area. The data are averaged over the period of 9 a.m. to 6 p.m. except from 12 p.m. to 1 p.m. The variation of the lighting plus plug loads decreases as the floor area increases. This relationship is stochastically modeled in the section “Methodology for deriving percentiles of internal heat gains.”

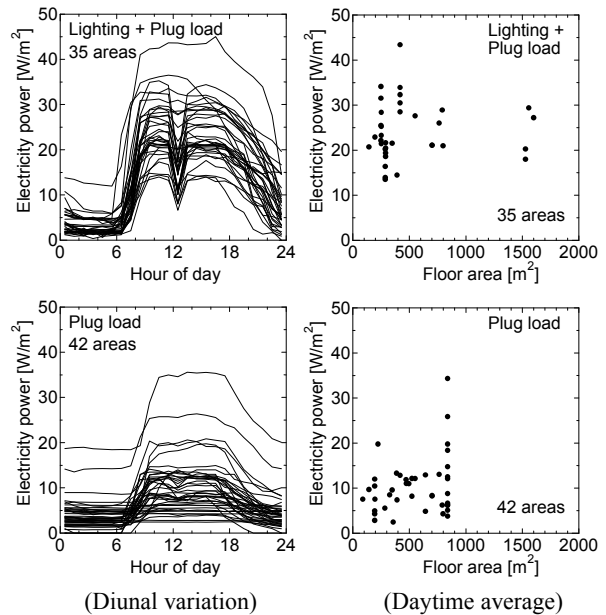


Figure 4 Diurnal variation and daytime average of internal heat gains (All buildings)

Probability distribution of time-averaged daytime internal heat gains (Building No. 6)

In Figure 4 (lower right), some plotted points form a vertical line at a floor area of approximately 800 m². These points come from measurements in Building No. 6. To identify the probability distribution, we plot these points on a probability chart for a lognormal distribution, as shown in Figure 5. In this figure, the horizontal axis, $\Phi^{-1}(p)$ is the inverse of the cumulative probability function for a standard normal distribution (e.g., $\Phi^{-1}(0.5) = 0$) where p is the cumulative probability. To derive the scatter plot, we sorted measurement values [W/m²] in ascending order, and calculate the cumulative probability for each measurement value. For example, the i^{th} -smallest measurement value gives the cumulative probability of $i/(N+1)$ where N is the number of the measurements. The vertical axis is the logarithm of the random variable, i.e. the internal heat gain in this case. Thus, the scattered points are linearly distributed if the probability distribution can be approximated to a log-normal distribution.

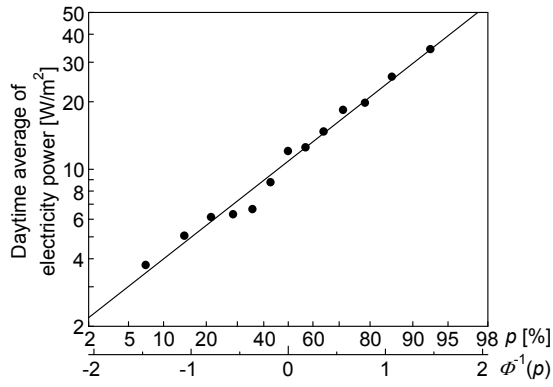


Figure 5 Probability plot for lognormal distribution (Building No. 6)

The points in Figure 5 approximate a straight line, which means that the variation of the plug loads conforms to a lognormal distribution when the floor areas are the same. It is preferable to collect more data from various types of buildings to identify the probability distribution, but we assume a log-normal distribution for the internal heat gain at the same floor area henceforth.

METHODOLOGY FOR DERIVING PERCENTILES OF INTERNAL HEAT GAINS

We present a method for deriving the percentiles of daytime internal heat gains. A percentile is the value of internal heat gain below which a certain percent of observations falls. As seen in Figure 4 (upper right), the variation of daytime internal heat gains decreases with the increase of floor area. Thus, percentiles need to be calculated for each floor area.

Stochastic model

Based on Figure 5, we assume that the variation of internal heat gains conforms to a lognormal distribution when their floor areas are the same. Thus, the probability density function of internal heat gains at a floor area of A [m²] is represented as follows:

$$f_A(x) = \frac{1}{\sqrt{2\pi}\zeta(A)x} \exp\left[-\frac{1}{2}\left(\frac{\ln x - \lambda(A)}{\zeta(A)}\right)^2\right] \quad (1)$$

Here, x is the value of the random variable, i.e., the internal heat gain per area in this case, and λ and ζ are parameters that represent the following statistics.

$$\lambda(A) = E(\ln x) \quad (\text{at floor area } A) \quad (2)$$

$$\zeta(A) = \{Var(\ln x)\}^{1/2} \quad (\text{at floor area } A) \quad (3)$$

Here, E and Var are mean and variance operators, respectively.

To provide a versatile model applicable to various floor areas, we introduce two parameters, α and ζ_0 ($=\zeta(A_0)$). We can calculate $\lambda(A)$ and $\zeta(A)$ in Equation (1) by the following equations, given the two parameters, α and ζ_0 .

$$\sigma^2(A_0) = \mu^2(\exp(\zeta_0^2) - 1) \quad (4)$$

$$\sigma^2(A) = \left(\frac{A_0}{A}\right)^\alpha \sigma^2(A_0) \quad (5)$$

$$\zeta(A) = \sqrt{\ln\left(1 + \frac{\sigma^2(A)}{\mu^2}\right)} \quad (6)$$

$$\lambda(A) = \ln \mu - \frac{1}{2}\zeta^2(A) \quad (7)$$

Here, A_0 is a reference area, which can be selected arbitrarily; μ is the mean of the internal heat gain; $\sigma^2(*)$ is its variance at the floor area of *. We assume $\mu (=E(x))$ is constant with floor area, and estimate it by averaging all sample data. Equations (4), (6), and (7) are general formulas for the lognormal distribution. Equation (5) represents the reduction in variance with the increase in floor area. The variance decreases rapidly when parameter α is a large value, such as 1.0. The value 1.0 means that the internal heat gain in a space is independent from the adjacent spaces. On the other hand, the variance decreases slowly when α is small, and the variance is constant when α is 0. Here, the value of 0 means that the internal heat gains in a space completely correlates to that in the adjacent spaces. Thus, the possible range of α is from 0 to 1.

Bayesian method for deriving posterior distribution of unknown parameters

We use the Bayesian method for estimating the probability distribution of the unknown parameters, α and ζ_0 . The Bayesian method revises the probability density function with additional information related to unknown parameters, and the equation is schematically represented as follows.

(Posterior probability distribution)

$$\propto (\text{Prior distribution}) \times (\text{likelihood}) \quad (8)$$

where the likelihood is a function of the unknown parameters and gives the probability density of the observed outcomes, i.e., the combination of the values of observed daytime internal heat gains, given the values of α and ζ_0 . Equation (8) is rewritten for our problem as follows.

$$f_{pos}(\alpha, \zeta_0) = f_{pri}(\alpha, \zeta_0) \times \prod_{i=1}^N f_{A_i}(Q_i, \alpha, \zeta_0) \quad (9)$$

where f_{pos} , f_{pri} are the posterior and prior probability density functions, given the parameter values of α and ζ_0 ; i is an index that identifies the observation of internal heat gains; N is the number of spaces for observations; and Q_i is the observed daytime-averaged internal heat gain in i^{th} space; $f_{A_i}(Q_i, \alpha, \zeta_0)$ is the likelihood, i.e., the conditional probability density of an observation being equal to Q_i , given the parameter values of α and ζ_0 . The value of $f_{A_i}(Q_i, \alpha, \zeta_0)$ is calculated by substituting the value of Q_i for x into Equation (1) after applying Equations (4) to (7).

MCMC method for deriving percentiles of internal heat gains

The percentile of an internal heat gain that conforms to a lognormal distribution is derived from the following equation.

$$x_p(A) = \exp(\lambda(A) + \zeta(A)\Phi^{-1}(p)) \quad (10)$$

where x_p is the value of the internal heat gain below which p percent of the observations fall.

We can calculate the percentile at a certain floor area by Equation (10), given the values of α and ζ_0 , because λ and ζ in Equation (10) are derived from Equations (4) to (7). However, α and ζ_0 are assumed to be stochastic parameters in this paper; thus, the percentile is also a stochastic variable. We use the MCMC method to obtain the mean and the S.D. of the percentile. The MCMC sampling is a form of Monte Carlo simulation and generates sampled series of stochastic parameters that conform to a known probability distribution. In this study, we can derive a series of parameter combinations of α and ζ_0 that conform to the posterior distribution expressed by Equation (9).

The mean and the S.D. of the percentile are derived by calculating the sample mean and the sample S.D. of x_p in Equation (10), directly with use of the parameter series generated by the MCMC sampling.

The reason for using Bayesian and MCMC method

It was possible to use maximum-likelihood method to derive percentiles of internal heat gains. In that case, a certain type of optimization method would be used to determine the combination of α and ζ_0 that maximizes the likelihood, L , which is represented as

$$L = \prod_{i=1}^N f_{A_i}(Q_i, \alpha, \zeta_0) \quad (11)$$

where the notation of the right-hand side is the same as Equation (9). The optimization would give the maximum likelihood solution, but could not give the uncertainty of the estimated parameters.

MCMC method with Bayesian approach is used in this paper because the methodology estimates probability density represented in Equation (9) rather than the most probable point of parameters. With use of MCMC method, we can check the uncertainty of the estimated parameters as well as deriving the means of percentiles.

ANALYSIS RESULTS FOR LIGHTING PLUS PLUG LOADS

We apply the methodology described above to the observed data of the lighting and plug loads in the 35 spaces listed in Table 1.

Calculation settings

The target data are derived by averaging the lighting plus plug loads [W/m^2] from 9 a.m. to 6 p.m. (except

for the 12 p.m. to 1 p.m. lunch hour) for each measured space. Those data coincide with the plots in Figure 4 (upper right). The average of those data, μ , is 24.10 W/m^2 , and this value is used when Equations (4), (6), and (7) are applied. Reference area A_0 is set to $1,000 \text{ m}^2$.

A uniform distribution over the interval $[0, 1]$ is assumed for the prior distribution of α . An inverse-gamma distribution is assumed for the prior distribution of ζ_0^2 . An inverse-gamma distribution has two parameters: the shape parameter and the scale parameter. We set 0.01 for both of these parameters, and so the value of ζ_0^2 is almost uncertain before the observations are available.

The starting values of the parameters in the MCMC method are 0.4 for α , and 0.3 for ζ_0 , respectively. We use the Metropolis–Hastings algorithm for the MCMC method and generate a proposed sample parameter (α', ζ_0') from the proposed density, $P((\alpha', \zeta_0') | (\alpha_t, \zeta_0, t))$, which suggests a new sample parameter (α', ζ_0') given the present sample parameter (α_t, ζ_0, t) . We employ a two-dimensional Gaussian distribution for P , centered at (α_t, ζ_0, t) with an S.D. of 0.10 for α and 0.03 for ζ_0 . The random variables of α' and ζ_0' from the proposed density, P , are independent each other. The number of samplings is 10,000, and the first 2,000 points are discarded to avoid the effect of the starting sampling point.

Posterior distribution of parameters

Prior to carrying out the MCMC sampling, we examine the posterior distribution of parameters α and ζ_0 (Figure 6). This figure is derived by assigning the values of (α, ζ_0) at the grid points of an orthogonal lattice to Equation (9). The values of the vertical axis are relative because we do not consider the normalization constant that makes the posterior density integrate to the value 1.

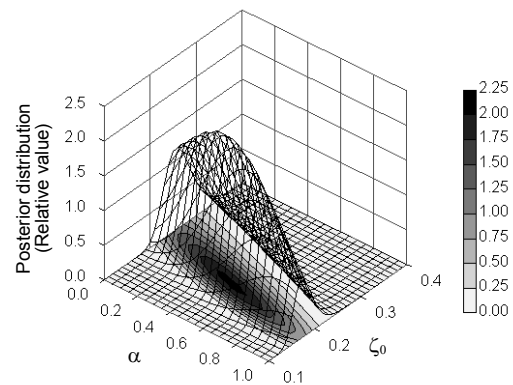


Figure 6 Posterior distribution for parameters α, ζ_0

According to this figure, the value of ζ_0 is distributed narrowly around approximately 0.2. However, α is distributed widely from 0 to 1, which implies that the value of α cannot be estimated with a high degree of accuracy.

Parameter estimation by MCMC

Figure 7 shows the sampling points generated by the MCMC method. The distribution of the sampling points is consistent with that of Figure 6, which suggests the MCMC sampling works properly.

Statistics such as the mean and the S.D. of parameters α and ζ_0 are directly calculated by using the sampling points except the first 2,000 points.

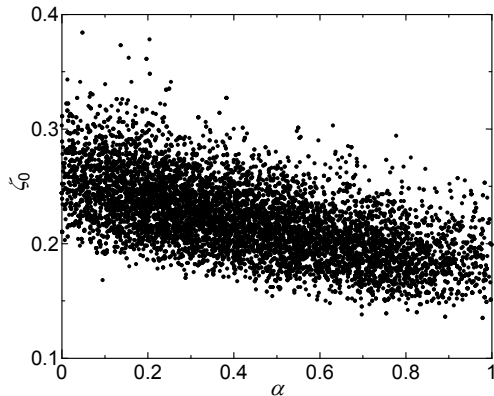


Figure 7 Sampling points derived by MCMC method

Table 2 Statistics related to parameters α , ζ_0

	α	ζ_0
Mean	0.431	0.220
Median	0.413	0.217
Standard deviation	0.255	0.034

Table 2 shows the statistics derived. Again, the obtained S.D. is large for α and small for ζ_0 . Parameter ζ_0 determines the variability around the mean value, μ , at the reference floor area of A_0 , and α determines how rapidly the variability decreases with the increase of floor area. The obtained S.D. implies that the variability around the mean can be estimated with relatively high accuracy, but the estimation of the decreasing rate is not so reliable.

Percentile of lighting plus plug loads

Finally, we present the percentiles of the lighting plus plug loads in relation to floor area. Figure 8 shows the mean of the percentiles. Here, the mean values are derived by computing the average of $x_p(A)$ in Equation (10) taken over the last 8,000 sampling points of (α, ζ_0) .

The value of the 95th percentile is approximately 41 W/m² at a floor area of 100 m², which is 1.7 times higher than the average. The 95th percentile decreases with the increase of floor area and is approximately 30 W/m² at 10,000 m². We can use 41 W/m² for the peak cooling load calculation to determine the cooling capacity of an air-handling unit that covers a workspace of 100 m². In contrast, we can reduce the setting of the internal heat gain to 30

W/m² for determining the cooling capacity of chillers that cover the whole building of 10,000 m² with the same exceedance probability. In other words, setting the value of the internal heat gain constant, no matter what the floor area is, gives a higher risk of overload for an air-handling unit than for a chiller.

In Japan, we commonly ignore the internal heat gain for calculating the peak heating load. However, Figure 8 suggests that 10 to 20 W/m² of the internal heat gain can be anticipated as a heat source that leads to the reduction of the heating capacity of the air handler, boiler, etc.

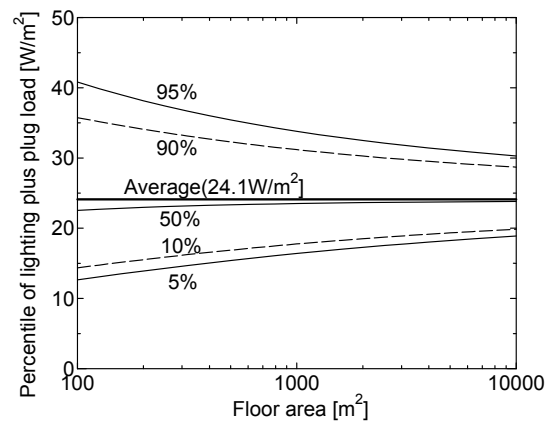


Figure 8 Mean of percentile of lighting plus plug loads in relation to floor area

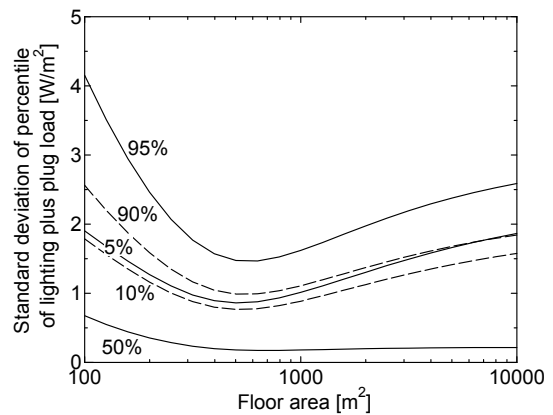


Figure 9 Standard deviations of percentile of lighting plus plug loads in relation to floor area

The number of data used to calculate the percentile is relatively small at 35, and so the reliability needs to be examined. Figure 9 shows the S.D.s of the percentiles, which are derived by computing the S.D. of $x_p(A)$ in Equation (10) taken over sampling points. According to this figure, S.D. for the 50th percentile or median, is lower than 1 W/m² and demonstrates high accuracy. In contrast, higher percentiles such as the 90th and 95th percentiles have lower reliability because their S.D.s are higher. The reliability is high at approximately 500 m² and low at smaller or larger floor areas. One reason for the difference is that the scale of the measured spaces is concentrated at the

medium floor area of approximately 500 m². We need to collect more measured data of smaller or larger spaces, and add these to the estimation procedure to improve the accuracy of the percentiles of internal heat gains.

CONCLUSIONS

We proposed a methodology for deriving a certain percentile of daytime averaged internal heat gain in a workspace, given the floor area. To demonstrate the methodology, we applied it to the total of lighting and plug loads measured in 35 workspaces in Japanese offices.

The methodology is also applicable to a plug load only, or to other internal heat gains, such as the number of people in the space. By using the derived percentile, we can determine a setting value of the internal heat gain for calculating the peak cooling/heating load. The setting values can be different depending on the HVAC equipment because the covered floor area differs according to the equipment. The difference is reasonable in terms of equal risk for an overload of each item of equipment. The capacity of central heat source such as chillers or boilers would be reduced if the overload risk is adjusted to be equal to that of terminal units. In that case, equipment characteristics, especially part load performance, should be considered to figure out the amount of energy and cost reduction.

To improve the accuracy of the derived percentile, it is necessary to collect more data, especially in small or large floor areas. Moreover, the derived chart is valid only when no other information related to internal heat gain is available. If we know in advance the design value of the electricity capacity for the lighting or plug load, the percentile must change accordingly. We need to modify the methodology to consider such prior knowledge.

ACKNOWLEDGEMENT

We would like to thank the project team at SHASE, Tokyo for their contribution to this research, and Dr. Takaharu Kawase, professor of Chiba University, for providing data of internal heat gains to us for our analysis.

REFERENCES

- Abushakra, B., Sreshthaputra, A., Haberl, J.S., Claridge, D.E. 2001. Compilation of Diversity Factors and Schedules for Energy and Cooling Load Calculations, ASHRAE Research Project 1093-RP, Final Report, Energy Systems Laboratory, Texas Engineering Experiment Station, Texas A&M University System, Texas, USA.
- Akiba, T., Nobe, T., et al. 2004. Investigation of Renovated Office Building (Part2 Investigation of Working Situation and Electrical-Demand in Office), Summaries of Technical Papers of Annual Meeting D-2, pp.1233-1234, Architectural Institute of Japan (AIJ), Hokkaido, Japan. (in Japanese)
- Akiba, T., Nobe, T., et al. 2005. Investigation of Renovated Office Building (Part5 Investigation of Working Situation and Electrical Demand in Office), Summaries of Technical Papers of Annual Meeting D-2, pp.1255-1256, AIJ, Kinki, Japan. (in Japanese)
- ASHRAE. 2009. 2009 ASHRAE Handbook - Fundamentals SI Edition, American Society of Heating, Refrigerating and Air-Conditioning Engineers, Inc., Atlanta, GA, USA.
- Kawase, T., Yagita, Y. 2005. Study on energy consumption of OA equipments in an office building, Technical Papers of Annual Meeting, pp.1149-1152, AIJ, Hokkaido, Japan. (in Japanese)
- Pedersen, L. 2007. Load Modelling of Buildings in Mixed Energy Distribution Systems, Doctoral thesis, Norwegian University of Science and Technology, Trondheim, Norway.
- Pedersen, L., Stang, J., Ulseth, R. 2008. Load prediction method for heat and electricity demand in buildings for the purpose of planning for mixed energy distribution systems, Energy and Buildings, Vol.40, pp.1124-1134.
- Saldanha, N., Morrison, I.B. 2012. Measured end-use electric load profiles for 12 Canadian houses at high temporal resolution, Energy and Buildings, Vol.49, pp.519-530.
- SHASE. 2008. Internal Heat Gains in Office Building and Thermal Load Calculation, Report R1009-2008, The Society of Heating, Air-Conditioning and Sanitary Engineers of Japan. (in Japanese)
- SHASE. 2011. Field Investigation of Internal Heat Gains, Space Usage, and Thermal Load/HVAC System Simulation, Report R 1018-2011, The Society of Heating, Air-Conditioning and Sanitary Engineers of Japan. (in Japanese)
- Shinkawa, T., Nobe, T. 2006. Time Series Data from Internal Load Factors in Offices, Summaries of Technical Papers of Annual Meeting D-2, pp.1167-1168, AIJ, Kanto, Japan. (in Japanese)
- Tokyo Denki Univ., The Univ. of Tokyo, Okayama Univ. of Science, Chiba Univ., Tokyo Univ. of Science, SHASE. 2010. Basic Research on Estimation Method of Energy Consumption of Commercial Buildings, Research report funded by Ministry of Land, Infrastructure, Transport and Tourism. (in Japanese)
- Wilkins, C.K. 1998. Electronic Equipment Heat Gains in Buildings, ASHRAE Transactions, Vol. 104, pt. 1A.